

A NOVEL DIRECT TORQUE CONTROL USING DUTY CYCLE CONTROL FOR TORQUE RIPPLE REDUCTION BY MATRIX CONVERTER-FED PMSM DRIVES



Allam Jyothikishore¹, S.Ramesh²

PG Student [PE&ED], Dept. of EEE, SISTK, jyothikishore.allam@gmail.com,India¹

Associative professor, Dept. of EEE, SISTK,Swamiramesh20@gmail.com,Andhra Pradesh, India²

Abstract— A novel direct torque control (DTC) strategy utilizing obligation cycle optimization is proposed for matrix converter(MC)-predicated sempiternal-magnet synchronous motor (PMSM)drive system, which is characterized by low torque ripples, no desideratum for rotational coordinate transformation, and fine-tuned switching frequency. Analytical expressions of change rates of torque and flux of PMSM as a function of MC voltage vectors are derived. An enhanced switching table is established by betokens of discretization and averaging, in which changes of torque and flux caused by voltage vectors are shown explicitly. Then, the proposed MC-victualued DTC algorithm is implemented predicated on the table. Numerical simulation and experiments with a prototype are carried out. Both simulation and experimental results demonstrate that remarkable torque ripple reduction, more than 30%, has been achieved. As a result, the proposed strategy is proved to be efficacious in reducing torque ripples for MC-predicated PMSM drives.

Key words—Direct torque control (DTC), matrix converter(MC), permanent-magnet synchronous motor (PMSM), torque ripple reduction

I. INTRODUCTION

Matrix converters (MCs) are a kind of compact ac-ac converters without an intermediate dc link. It is magnetizing extensive attention due to their advantages such as high power density, sinusoidal input/output currents, and controllable input power factor [1]. Recently, research works on commutation technology [2], operation stability [3], and control/modulation strategy [4]–[18] of MCs have

been widely reported. Driven by the achievements of these research works, MCs have been increasingly applied in many industrial fields, such as elevators, wind power generation, and mechanical manufacture [19].A substantial amount of research fixating on control and modulation strategies of MCs, developed up to now, can be divided into scalar techniques, pulse width modulation (PWM), predictive control, and direct torque control (DTC) [4].DTC was introduced into voltage source inverter (VSI)-victualued induction machines.

II. STANDARD MC-DTC

A. MCs

A typical three-phase to three-phase MC with nine bidirectional switches is shown in Fig. 1. The relationship between the input and output voltage and current of MC can be expressed as

$$v_o = \begin{bmatrix} v_A \\ v_B \\ v_C \end{bmatrix} = \begin{bmatrix} s_{Aa}(t) & s_{Ab}(t) & s_{Ac}(t) \\ s_{Ba}(t) & s_{Bb}(t) & s_{Bc}(t) \\ s_{Ca}(t) & s_{Cb}(t) & s_{Cc}(t) \end{bmatrix} \begin{bmatrix} v_a \\ v_b \\ v_c \end{bmatrix} = M \cdot v_i \quad (1)$$

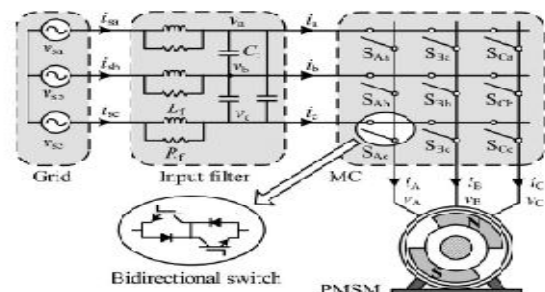


Fig. 1. Simplified circuit of a three-phase to three-phase MC.

$$\frac{d}{dt} T_e = K(v_y - \omega_r |\Psi_s|) \quad (8)$$

Where θ_s and θ_r are the stator and rotor positions, respectively, and ω_r is the rotor electrical angular velocity. From (6), (8), and (9), the change rate of torque can be derived as

$$V_{+1x} = \frac{2}{3v_{ab} \cos(-\theta_s)} = 2/\sqrt{3}V_m \cos(\alpha_i + \frac{\pi}{6}) \cos \theta_s \quad (9)$$

$$V_{+1y} = \frac{2}{3v_{ab} \sin(-\theta_s)} = -2/\sqrt{3}V_m \cos(\alpha_i + \frac{\pi}{6}) \sin \theta_s \quad (10)$$

where $K = (3p/2LdLq)[\psi fLq \cos \delta - \Psi_s/(Lq - Ld) \cos 2\delta]$. According to (5) and (10), it can be noticed that the change rates of flux and torque of PMSMs are related to the x-axis and y-axis components of the stator voltage vector, respectively.

B. Evaluation Function of Torque and Flux

Each output voltage vector of MCs can be decomposed into x and y components. Take the +1 switching state as an example ,its voltage vector projected on frame x-y is presented, the stator flux vector is oriented and aligned on the x-axis, the a-axis denotes the A phase windings of motors, θ_s is the stator flux linkage position, and V +1 is the active voltage vector engendered by the +1 switching state. A scan be noted from Table I, the x-y components of V +1 can be expressed as

$$\tau = \frac{V_y}{2/\sqrt{3}V_m} \quad (11)$$

$$\lambda = \frac{V_x}{2/\sqrt{3}V_m} \quad (12)$$

$$e = \frac{\omega_r |\Psi_s|}{2/\sqrt{3}V_m} \quad (13)$$

It can be noted that both τ and λ are cognate to the voltage vector, and e is cognate to motor speed. Superseding (11) into (12) and (13), the torque evaluation function and flux evaluation function of the +1 switching state are obtained as

$$\tau_{+1} = -\cos(\alpha_i + \frac{\pi}{6}) \sin \theta_s \quad (14)$$

$$\lambda_{+1} = \cos(\alpha_i + \frac{\pi}{6}) \cos \theta_s \quad (15)$$

The τ and λ functions of all active voltage vectors of MC scan be calculated predicated on the aforementioned contents, and the results are shown in

the right side of Table I. By superseding (12)–(14) into (10) and (5), the cognation ship between the evaluation functions τ , λ , and e and the vicissitude rates of torque and flux can be obtained as

$$\frac{d}{dt} T_e \propto K(\tau - e) \quad (16)$$

$$\frac{d}{dt} |\Psi_s| \propto \lambda \quad (17)$$

MCs have 18 active switch states, which correspond to 18pairs of τ and λ functions. From (17) and (18), the common features of all the τ and λ functions can be concluded as follows: τ and λ functions are proportional to the change rates of torque and flux, respectively.

IV. NOVEL MC-DTC

A. Enhanced MC Switching Table

As the online calculation of the functions of τ and λ according to Table I will bring undesirable calculation burden ,a lookup table with the average values of τ and λ can eliminate the burden by explicitly showing the effects of MCs voltage vectors on torque and flux .It can be noted that both τ and λ are binary periodic functions. An analysis of one period, where $\theta_s \in [0, 2\pi]$ and $\alpha_i \in [0, 2\pi]$, will be carried out.

$$p_r = \text{round} \left[\frac{k}{(\frac{\pi}{6})^2} \int_{\frac{\pi}{6}(l_\alpha-1)}^{\frac{\pi}{6}l_\alpha} \int_{\frac{\pi}{6}(l_\theta-1)}^{\frac{\pi}{6}l_\theta} \tau d\theta_s d\alpha_i \right] \quad (18)$$

$$p_\lambda = \text{round} \left[\frac{k}{(\frac{\pi}{6})^2} \int_{\frac{\pi}{6}(l_\alpha-1)}^{\frac{\pi}{6}l_\alpha} \int_{\frac{\pi}{6}(l_\theta-1)}^{\frac{\pi}{6}l_\theta} \lambda d\theta_s d\alpha_i \right] \quad (19)$$

where round[] denotes the rounding of the number to the most proximate integer and p_r and p_λ are the impact factors of torque and flux, respectively. The values of p_r and p_λ will be integers between -9 and +9 when the coefficient k is equipollent to 10. According to (17)–(20), the relationships of p_r and p_λ with the transmutation rates of torque and flux can be obtained as follows:

$$\frac{d}{dt} T_e \approx \text{avg} \left(\frac{d}{dt} T_e \right) \propto K(p_r - p_e) \quad (20)$$

$$\frac{d}{dt} |\Psi_s| \approx \text{avg} \left(\frac{d}{dt} |\Psi_s| \right) \propto p_\lambda \quad (21)$$

where $avg(\)$ is the average function in each zone and the back EMF impact factor p_e is

$$p_e = round(10e) \quad (22)$$

equations (21) and (22) implicatively insinuate that p_r and $p\lambda$ are approximately proportional to the transmutation rates of torque and flux, respectively.

Superseding (15) into (19), the p_r of the V +1 vector in each zone can be calculated. Moreover, the enhanced switching table of the V +1 vector can be established, as presented in Fig. 6, in which the effects of the +1 switching state on torque can be shown explicitly. If the table is colored in accordance with the transmuting of p_r , the kindred attribute is evident .

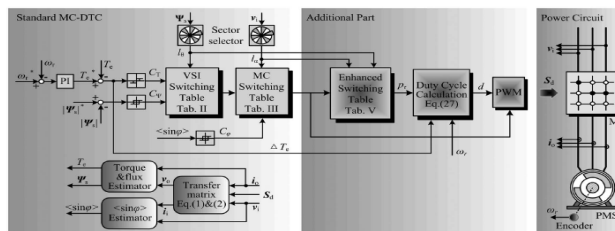


Fig. 3. Proposed MC-DTC block diagram.

he torque and flux impact factors p_r and $p\lambda$ in the enhanced switching table are integers ranging from -9 to +9, except 0, ±4, ±7, and ±8. The reason is that ±4, ±7, and ±8 are cognate to the rotating switching states of MCs and 0 is engendered by the zero switching states of MCs. In such a way, the effects of all the active switching states of MCs on the torque and flux of PMSMs according to the enhanced switching table can be evaluated explicitly.

B. Calculation of Obligation Cycle

According to (21), the vicissitude rates of torque engendered by active vectors and zero vectors are approximately proportional to $K(p_r - p_e)$ and $-Kp_e$, respectively. Supposing that an active vector is applied to the motor with a time duration of t_k in one control cycle t_s , the impact of this active vector on motor torque can be obtained as follows:

$$\Delta T_e' = k_\tau K(p_r - p_e)t_k \quad (23)$$

where k_τ is a positive constant. A zero voltage is applied for the rest time of the control cycle $t_s - t_k$; hence, the torque variations deduced as

$$\Delta T_e'' = -k_\tau K p_e (t_s - t_k) \quad (24)$$

The sum of (24) and (25) is the total torque increment in a full control cycle, presented as follows:

$$\Delta T_e = \Delta T_e' + \Delta T_e'' = k_\tau K(p_r t_k - p_e t_s) \quad (25)$$

where p_r is obtained by Fig. 6, p_e is calculated by (23), and ΔT_e is the difference between the reference and actual value of torque. Based on (26), the duty cycle can be derived as

$$d = \frac{t_k}{t_s} = \frac{\Delta T_e}{KT p_r} + \frac{p_e}{p_r} \quad (26)$$

where KT is the torque constant which equals $k_\tau K t_s$. The analysis about the value range of KT will be given in Section IV-C.

C. Analysis of Torque Constant KT

Theoretically, the torque constant KT equals $k_\tau K t_s$. According to (10), K is a function of angle δ and motor parameters. It tends to vary as a result of δ change caused by load ripple and motor parameter variation caused by the temperature rising or system nonlinear characteristic. Therefore, in this paper, KT is obtained by the experimental tuning method rather than through calculation by $k_\tau K t_s$. The qualitative analysis of the impact of KT variation on the performance of the proposed control method is given as follows.

$$\frac{1.2T_N}{KT p_r} \geq 0.85 \quad (28)$$

Where T_N is the motor rated torque and p_r is estimated to be 9.

2) To ensure small torque ripples in the system steady state, the former part in (27) should be 0.1 ~ 0.5 times the latter part, and we obtain

$$0.1 p_e \leq \frac{|BT_e|}{KT} \leq 0.5 p_e \quad (29)$$

Where BT_e is the torque hysteresis band and p_e is set to be 4. The value range of KT is the intersection of (28) and (29). In the range, with a larger value of KT , torque ripples in the steady state are less, but dynamic performance is degraded. Moreover, with a

smaller value of KT , fast dynamic response is achieved ,but torque ripples are significant.

D. Proposed MC-DTC

The block diagram of the proposed MC-DTC is presented in Fig. 3. It can be optically discerned that an enhanced switching table and an obligation cycle calculation part are integrated predicated on the standard method. At first, an active voltage vector is culled utilizing the standard method; then, $\rho\tau$ is obtained by referring to the enhanced switching table. At last, the obligation cycle is calculated by superseding $\rho\tau$ and motor speed into (27).In Fig. 3, the stator flux estimator employs the low-pass filter method [28]. Its block diagram is shown in Fig. 8.In Fig. 8, ω_e is the synchronous frequency of the stator flux and ω_c is the cutoff frequency of the low-pass filter. The equations of ω_e and ω_c are presented as follows:

$$\omega_c = \gamma\omega_e, \omega_e = \frac{\psi_\alpha(u_\beta - R_S i_\beta) - \psi_\beta(u_\alpha - R_S i_\alpha)}{\psi_\alpha^2 + \psi_\beta^2} \quad (30)$$

. Aside from that, methods based on modern control theory can also be used for flux estimation, such as the self-adaptive estimator [29] and Kalman filter [30].Torque estimation is performed in the stationary $\alpha - \beta$ coordinate as follows:

$$T_e = 1.5p(\psi_\alpha i_\beta - \psi_\beta i_\alpha) \quad (31)$$

$$\sigma_T = \sqrt{\frac{1}{n-1} \sum_{i=1}^n (T_e(i) - \overline{T_e})^2}, \overline{T_e} = \frac{1}{n} \sum_{i=1}^n T_e(i) \quad (32)$$

The performances of the standard and proposed methods are given and compared by Matlab /Simulink. The parameters of the PMSM, control system, and input filter are presented in Tables V–VII, respectively. The sampling periods of the standard and proposed methods are set to be 50 and 100 μs ,respectively, in order to achieve kindred average commutation frequencies .The electromagnetic torque ripples of both the standard and the proposed methods are evaluated by betokens of their respective standard deviation, which can be expressed aswhere n is the number of samples .The dynamic performances of the standard and proposed methods are shown in Fig. 4, where a step speed command(from 20 to 60 r/min) is introduced at $t = 1$ s, and then, an abrupt change of load (from 0 to 400

N · m) is introduced at $t = 1.5$ s. It can be seen that both the standard and the proposed methods have fast torque dynamic response. How ever ,a remarkable torque ripple reduction can be observed in the proposed method. To be specific, the values of σT of the standard and proposed methods are 12.99 and 7.80 N · m, respectively, within the range of 1.3–1.5 s.In Fig. 10, robustness against motor parameter variation is tested for the proposed method. In the simulation, the d-q inductances are increased to 150% of their nominal values, and the other simulation conditions are the same as those in Fig. 9.

TABLE II
 COMPARISON BETWEEN IMPROVED MC-DTC

	Method I[10]	Method II[13]	Proposed method
number of vectors in one control period	one active vector or one zero vector	four active vectors and one zero vector	one active vector and one zero vector
motor parameters dependence	R_s, ψ_f	L_d, L_q, R_s, ψ_f	R_s, ψ_f
rotational coordinate transformation	not needed	needed	not needed
PWM	not needed	needed	needed
fixed switch frequency	unfixed	fixed	fixed
input current	worsened [10]	significantly improved [13]	slightly improved

TABLE III
 PARAMETERS OF CONTROL SYSTEM

Flux hysteresis bands	$B \Psi_s $	$\pm 0.5\% \psi_f$
<sin θ >hysteresis bands	$B\langle \sin\theta \rangle$	0
Torque hysteresis bands	BT_e	$\pm 1\% T_N$
Flux reference	$ \Psi_s ^*$	1.67 Wb
Torque constant (proposed method only)	K_T	8.5 Nm

It can be seen that the variation of motor inductance has no significant effect on system performance. Within the range of 1.3–1.5 s, the value of σT is equal to 5.78 N · m.

V. SIMULATION RESULTS

To verify the feasibility and efficacy of the proposed method, an MC setup was implemented, as shown in Fig. 12.The consummate system was connected to the utility grid through the variac. An input R–L–C filter was adopted to attenuate switching harmonics. A clamp circuit was designed to bulwark the MC against the over current and overvoltage that occur on the input side and/or output side of MC. The control system employed a TMS320F28335 digital signal processor for control strategy and an EP1C6 field-

programmable gate array for switch commutation. The sampling periods of the standard and proposed methods are 50 and 100 μ s, respectively. The parameters of the experimental system are presented in Tables V–VII.

A. Steady-State Performance

The steady performances of two methods are presented with the speed reference value being 40 r/min and the load torque being 150 N · m. In the experiment, the standard and proposed methods are implemented under kindred average commutation frequencies, which are identically tantamount to 4.44 and 4.84 kHz, respectively. The average commutation frequency is calculated by counting the total commutation numbers of a bidirectional switch during a fine-tuned period of time. Fig. 13 shows the electromagnetic torque, stator current, and stator flux modulus waveforms of two methods. Consequential torque ripple can be found in the standard method as shown in Fig. 5(a) with σT being 11.32 N · m, while Fig. 5(b) shows that remarkable torque ripple reduction can be found in the proposed method with σT being only 7.53 N · m.

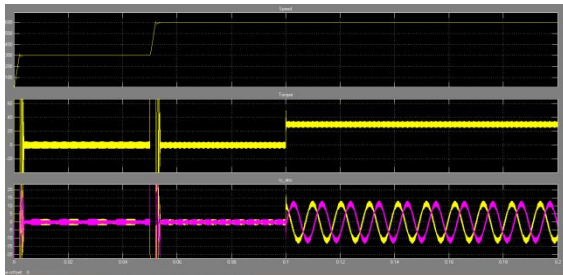


Fig. 4. Simulation results of transient performance. (a) Speed, electromagnetic torque, and stator current for standard method..

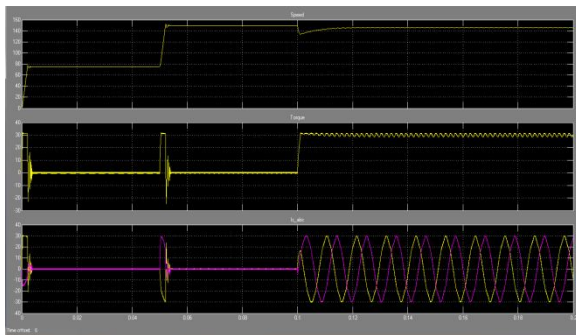


Fig. 5. Simulation results of speed, electromagnetic torque, and stator current for proposed method with 1.5Ld and 1.5Lq.

seen that the distortion of input current in the standard method is more severe than that in the proposed method. The THDs of the standard and proposed methods are 10.98% and 7.74%, respectively.

B. Dynamic Performance

Fig. 4 shows the waveforms of speed, electromagnetic torque, and stator current of two methods with the load torque stepping up from no load (approximately 30 N · m) to 200 N · m and the speed being 40 r/min. It can be seen that, with the abrupt change of load, for both the standard and the proposed methods, the electromagnetic torque increases rapidly, and the speed meets the reference value only after a short period. However, remarkable torque ripple reduction can be observed in the proposed method.

C. Low-Speed Behavior

Fig. 5 shows the waveforms of stator flux modulus and electromagnetic torque of the standard and proposed methods, respectively, with the speed being 15 r/min. In the experiment, against the variation of control parameters. To summarize, the experimental results are in accordance with the analysis in the previous section, the value of K_T is equal to 8.5 N · m, and the load torque steps up from no load to 150 N · m with different speed references. It can be seen that the proposed method is able to achieve better steady-state and dynamic performances with different operating conditions when an appropriate value is assigned to K_T .

VI. CONCLUSION

In this paper, a novel DTC algorithm utilizing obligation cycle control strategy has been proposed for MC-alimented PMSM drive system. This paper defines the evaluation functions to analyze the relationships between the voltage vectors of MCs and the transmutation rates of torque and magnitude of stator flux. By discretizing and averaging evaluation functions, the torque and flux impact factors p_t and p_λ are acquired, and they are approximately proportional to the vicissitude rates of torque and magnitude of stator flux, respectively. Furthermore, an enhanced switching table is established, and an incipient obligation cycle optimization approach is proposed. The performance of the novel MC-DTC

has been tested by simulation and experiment, and the results are concluded as follows.

1) Remarkable torque ripple reduction and expeditious dynamic replication can be achieved by the proposed method. The standard deviation of electromagnetic torque is reduced by more than 30%, compared with the standard method.

2) For low-speed range, distortions of stator flux can be eliminated to some extent compared with the standard

method. Therefore, the load capacity of the drive system is ameliorated by the proposed method.

3) The value of torque constant K_T can affect the performance of the proposed method. To discuss the influence

of K_T , an experimental tuning method of K_T is presented in this paper. Both theoretical analysis and experimental

results show that, with a more immensely colossal value of K_T , torque ripples in the steady state are less but dynamic performance

is degraded.

REFERENCES

- [1] P. W. Wheeler, J. Rodriguez, J. C. Clare, L. Empringham, and A. Weinstein, "Matrix converters: A technology review," *IEEE Trans. Ind. Electron.*, vol. 49, no. 2, pp. 276–288, Apr. 2002.
- [2] H. She, H. Lin, B. He, X. Wang, L. Yue, and X. An, "Implementation of voltage-based commutation in space-vector-modulated matrix converter," *IEEE Trans. Ind. Electron.*, vol. 59, no. 1, pp. 154–166, Jan. 2012.
- [3] C. Xia, P. Song, T. Shi, and Y. Yan, "Chaotic dynamics characteristic analysis for matrix converter," *IEEE Trans. Ind. Electron.*, vol. 60, no. 1, pp. 78–87, Jan. 2013.
- [4] J. Rodriguez, M. Rivera, J. Kolar, and P. Wheeler, "A review of control and modulation methods for matrix converters," *IEEE Trans. Ind. Electron.*, vol. 59, no. 1, pp. 58–70, Jan. 2012.
- [5] M. Venturini, "A new sine wave in sine wave out, conversion technique which eliminates reactive elements," in *Proc. Powercon 7*, 1980, pp. E3/1–E3/15.
- [6] X. Wang, H. Lin, H. She, and B. Feng, "A research on space vector modulation strategy for matrix converter under abnormal input-voltage conditions," *IEEE Trans. Ind. Electron.*, vol. 59, no. 1, pp. 93–104, Jan. 2012.
- [7] M. Rivera, A. Wilson, C. A. Rojas, J. Rodriguez, J. R. Espinoza, P. W. Wheeler, and L. Empringham, "A comparative assessment of model predictive current control and space vector modulation in a direct matrix converter," *IEEE Trans. Ind. Electron.*, vol. 60, no. 2, pp. 578–588, Feb. 2013.
- [8] S. Kouro, P. Cortes, R. Vargas, U. Ammann, and J. Rodriguez, "Model predictive control, a simple and powerful method to control power converters," *IEEE Trans. Ind. Electron.*, vol. 56, no. 6, pp. 1826–1838, Jun. 2009.
- [9] D. Casadei, G. Serra, and A. Tani, "The use of matrix converters in direct torque control of induction machines," *IEEE Trans. Ind. Electron.*, vol. 48, no. 6, pp. 1057–1064, Dec. 2001.
- [10] C. Ortega, A. Arias, C. Caruana, J. Balcells, and G. Asher, "Improved waveform quality in the direct torque control of matrix-converter-fed PMSM drives," *IEEE Trans. Ind. Electron.*, vol. 57, no. 6, pp. 2101–2110, Jun. 2010.
- [11] K.-B. Lee and F. Blaabjerg, "Sensorless DTC-SVM for induction motor driven by a matrix converter using a parameter estimation strategy," *IEEE Trans. Ind. Electron.*, vol. 55, no. 2, pp. 512–521, Feb. 2008.
- [12] J. Wang and J. Jiang, "Variable-structure direct torque control for induction motor driven by a matrix converter with overmodulation strategy," in *Proc. 6th IEEE IPEMC*, May 2009, pp. 580–584.
- [13] D. Xiao and M. F. Rahman, "Sensorless direct torque and flux controlled IPM synchronous machine fed by matrix converter over a wide speed range," *IEEE Trans. Ind. Informat.*, vol. 9, no. 4, pp. 1855–1867, Nov. 2013.
- [14] C. Xia, Y. Yan, P. Song, and T. Shi, "Voltage disturbance rejection for matrix converter-based PMSM drive system using internal model control," *IEEE Trans. Ind. Electron.*, vol. 59, no. 1, pp. 361–372, Jan. 2012.